

Article

# Advancing Photodynamic Therapy Efficiency on MCF-7 Breast Cancer Cells through Silica Nanoparticles-Safranin Encapsulation: In-Vitro Evaluation

Khaled Aljarrah <sup>1,\*</sup>, M-Ali H. Al-Akhras <sup>1</sup>, Ghaseb N. Makhadmeh <sup>1</sup>, Tariq AlZoubi <sup>2,\*</sup>, Majed M. Masadeh <sup>3</sup>, M. H. A. Mhareb <sup>4</sup>, Samer H. Zyoud <sup>5</sup> and Osama Abu Noqta <sup>6</sup>

<sup>1</sup> Bio-Medical Physics Laboratory, Department of Physics, Jordan University of Science and Technology, Irbid 22110, Jordan; alakmoh@just.edu.jo (M.-A.H.A.-A.)

<sup>2</sup> College of Engineering and Technology, American University of the Middle East, Egaila 54200, Kuwait

<sup>3</sup> Department of Pharmaceutical Technology, Faculty of Pharmacy, Jordan University of Science and Technology, Irbid 22110, Jordan

<sup>4</sup> Department of Physics, College of Science, Imam Abdulrahman Bin Faisal University, Dammam 31441, Saudi Arabia

<sup>5</sup> Nonlinear Dynamics Research Center (NDRC), Department of Mathematics and Sciences, Ajman University, Ajman P.O. Box 346, United Arab Emirates

<sup>6</sup> MEU Research Unit, Middle East University, Amman 11831, Jordan; osama1987ahmad@yahoo.com

\* Correspondence: kjarrah@just.edu.jo (K.A.); tariq.alzoubi@aum.edu.kw (T.A.)

**Abstract:** Efficient drug delivery to target tissue is a major challenge in many cancer treatment modalities. Silica nanoparticles (SiNPs) have been identified as an ideal drug carrier due to their unique properties. In Photodynamic therapy (PDT), one of the key challenges in utilizing photosensitizers (PS) lies in effectively delivering the PS to the targeted tissue. Using Silica nanoparticles encapsulation will effectively prevent the leakage of entrapped PS from the particles, protects against reduction by the retinal endothelial system, and reduces PS toxicity. In this study, Silica nanoparticles (SiNPs) were used as carriers for Safranin (SF) as a photosensitizer agent to treat MCF-7 breast cancer cells in vitro. The SiNPs nanoparticles were synthesized, and their size and shape were measured using Transmission Electron Microscopy (TEM). Cytotoxicity was evaluated for different concentrations of encapsulated and naked SF. The optimal concentrations and exposure times required to eliminate the MCF-7 under light (Intensity  $\sim 110$  mW/cm<sup>2</sup>, red laser) were determined. The results indicated that encapsulated SF by SiNPs exhibited higher efficacy than naked SF with a +50% concentration efficacy and +78% exposure time efficacy. This confirmed the superior ability of encapsulated SF to eliminate MCF-7 cells compared to naked SF. The use of synthesized silica nanoparticles loaded with SF improved photodynamic therapy by increasing the bioavailability of SF in the target cells. Our results demonstrate that SiNP encapsulation significantly improves the efficacy of SF in eliminating MCF-7 cells compared to bare SF. This study underscores the potential of SiNPs as a drug delivery system for photodynamic therapy and could pave the way for developing more effective cancer treatments.

**Keywords:** photodynamic therapy; safranin; silica nanoparticles; encapsulation; MCF-7 cells



**Citation:** Aljarrah, K.; Al-Akhras, M.-A.H.; Makhadmeh, G.N.; AlZoubi, T.; Masadeh, M.M.; Mhareb, M.H.A.; Zyoud, S.H.; Abu Noqta, O. Advancing Photodynamic Therapy Efficiency on MCF-7 Breast Cancer Cells through Silica Nanoparticles-Safranin Encapsulation: In-Vitro Evaluation. *J. Compos. Sci.* **2023**, *7*, 274. <https://doi.org/10.3390/jcs7070274>

Academic Editor: Francesco Tornabene

Received: 11 June 2023

Revised: 21 June 2023

Accepted: 25 June 2023

Published: 3 July 2023



**Copyright:** © 2023 by the authors. Licensee MDPI, Basel, Switzerland. This article is an open access article distributed under the terms and conditions of the Creative Commons Attribution (CC BY) license (<https://creativecommons.org/licenses/by/4.0/>).

## 1. Introduction

Photodynamic cancer therapy (PDT) has been considered a highly successful cancer treatment technique in recent years. In comparison to other cancer treatment techniques, PDT is both effective and has limited side effects. Several more effective photosensitizers have been discovered and utilized to achieve this improvement [1,2]. By activating a photosensitizer (PS) with light, PDT generates reactive oxygen species (ROS), ultimately leading to cell death [3,4]. In PDT therapy, a primary challenge is delivering sufficient photosensitizer to the targeted tissues, as insufficient delivery may lead to reduced production

of reactive oxygen species. As photosensitizer molecules travel to the target tissue, the retinal endothelial system consumes some of them. The use of silica nanoparticles for encapsulation will prevent PS leakage from the particles. This reduces PS toxicity and protects against reduction by the retinal endothelial system. Apparently, this can be attributed to the fact that the silica nanoparticles form a protective layer around the PS molecules, thereby preventing them from escaping and PS molecules from interacting with the environment, thus ensuring the formulation remains stable and less likely to degrade over time. Additionally, the nanoparticles act as a buffer, reducing the amount of PS absorbed by the body and thus decreasing its toxicity [5]. The delivery of photosensitizers by Silica nanoparticles (SiNPs) is highly efficient and prevents their absorption by macrophages [6–8]. Previous studies have shown that SiNPs can encapsulate photosensitizers and protect them during delivery [9,10]. SiNPs exhibit a range of advantageous attributes that render them highly suitable for integration into drug delivery systems. These desirable features encompass their capacity for synthesis at low temperatures, low polydispersity, minimal toxicity, remarkable biocompatibility, the potential to encapsulate photosensitizers within their interior surfaces, and the ability to bind biomolecules onto their exterior surfaces [11–14]. To overcome the challenges of delivering therapeutic agents effectively and efficiently, silica nanoparticles have emerged as promising carriers for photosensitizers. These nanoparticles not only provide a protective shield but also ensure the precise delivery of the photosensitizer to its intended target. This circumvents potential interactions with the body's defense mechanisms. This can be attributed to the fact that the mechanism by which encapsulated photosensitizers are targeted is based on passive accumulation through enhanced permeability and retention, as well as active targeting through interactions between the ligand and the receptor. This process ensures that the photosensitizers are delivered specifically to the target cancer cells. Consequently, therapeutic effectiveness is increased by delivering a suitable PS concentration to the target tissue [15]. Silica nanoparticles enable precise control over the photosensitizer loading and release, thereby maximizing its therapeutic efficacy [9,10]. The SF release mechanism of Si NPs involves the activation of encapsulated photosensitizer molecules that undergo changes when exposed to light. As a result of this activation process, a large amount of singlet oxygen is produced, which breaks or passes through the pores of the silica nanoparticles [16]. This innovative approach holds immense potential for transforming photodynamic therapy and enhancing its precision as a targeted treatment for cancer.

Safranin (SF), a phenazinium dye-derived photosensitizer, exhibits remarkable phototoxicity against tumor cells, making it a promising candidate for PDT. SF possesses several advantageous properties that make it suitable for PDT applications. Firstly, it demonstrates a high quantum yield of ROS generation when excited within the therapeutic window of 500–520 nm. This specific wavelength range ensures efficient activation of SF during PDT. Additionally, SF exhibits low toxicity in the absence of light, enhancing its safety profile as a therapeutic agent [17,18]. Furthermore, SF has found applications beyond PDT, particularly in the field of photo-oxidation of organic compounds [19–21].

References [15–17]. SF's versatility makes it a highly appealing option for diverse research domains, encompassing tissue structure, cellular studies, and investigations involving bacteria [22–24]. Furthermore, SF has been shown to be effective in inhibiting various microorganisms, including *Staphylococcus aureus*, *Escherichia coli*, *Shigella flexneri*, *Bacillus subtilis*, and bacteria associated with oral pathology [25–27]. Additionally, SF has demonstrated efficacy in mitochondrial oxidation processes [28–30]. Phenazines, including SF, have been identified as highly suitable photosensitizers for photodynamic therapy. This is primarily due to their strong absorption in the visible region of the electromagnetic spectrum, enabling efficient light absorption during treatment. Moreover, their interaction with biological substances further contributes to their effectiveness in PDT [29]. By utilizing SF's unique properties, researchers can explore its potential for advancing PDT as a targeted cancer treatment. The high ROS generation, low toxicity, and broad applicability of SF

make it a promising candidate for further investigation and optimization in the field of photodynamic therapy.

MCF-7 breast cancer cells are a serious global health concern due to treatment resistance and the persistence of the disease [29]. Despite the development of therapeutic strategies, current treatments are impeded by drug resistance and disease persistence [30,31]. New strategies are required to target and treat drug-resistant breast cancer cells and reduce the risk of relapse. Such strategies need to be developed to truly tackle the global health challenge posed by MCF-7 breast cancer cells. Therefore, innovative and powerful treatment approaches are needed to effectively eliminate these cells. Safety and simplicity are important factors to consider when developing novel therapeutic options. Research should be dedicated to exploring treatments that target MCF-7 cells while ensuring patient safety and ease of administration. Such treatments should also have minimal side effects and be cost-effective. Moreover, they should be tailored to the individual patient to ensure optimal efficacy. In addition, they should be designed to target the most aggressive forms of cancer and work to prevent the spread of MCF-7 cells to other parts of the body. Advanced methods are required to eradicate MCF-7 cells [32,33]. It is crucial to create new and effective treatment strategies to tackle this aggressive type of breast cancer. Consequently, there is a need for thorough research in order to create innovative therapeutic options that specifically target MCF-7 cells yet also ensure safety and ease of administration for patients. To guarantee optimal results, studies should focus on developing novel therapeutic options that concentrate on these cancerous cells and their safety and simplicity. Furthermore, the results of the research must be carefully evaluated in terms of safety, efficacy, and cost-effectiveness before they are implemented in clinical practice. This would ensure that MCF-7 cells are targeted in the most efficient and safe way possible.

This study aimed to investigate the potential of SiNPs as carriers for safranin (SF) in PDT targeting MCF-7 breast cancer cells. Specifically, the study focused on evaluating the impact of encapsulating SF within SiNPs on its effectiveness in MCF-7 PDT. To the best of our knowledge, this is the first investigation to explore the effects of SF encapsulation by SiNPs on MCF-7 cells. The study encompassed several key aspects. Firstly, the cytotoxicity of SF-SiNPs was assessed to determine their biocompatibility and ensure their suitability for use in PDT. Additionally, the optimal concentration and exposure duration of SF-SiNPs were determined to maximize their therapeutic effectiveness. Comparative evaluations were conducted between encapsulated SF and naked SF, examining their performance at different concentrations and exposure times to assess any differences in their efficacy against MCF-7 cancer cells. By encapsulating SF within SiNPs, the study aimed to enhance the targeted delivery of SF to MCF-7 cells and potentially improve the overall PDT outcome. Evaluating the cytotoxicity, optimal concentration, and exposure parameters of SF-SiNPs provides valuable insights into their potential as a powerful therapeutic approach for MCF-7 breast cancer. The novel findings from this study contribute significantly to the emerging field of nanomedicine-based cancer therapies by providing insight into the specific application of SF-SiNPs in MCF-7 PDT. It is intended that these findings will pave the way for further advancements in drug delivery systems and open up new avenues for the development of highly effective treatments for MCF-7 breast cancer.

## 2. Materials and Method

The encapsulation of SF by SiNPs was accomplished using the microemulsion technique [33], while the reverse-micellar method was utilized for the encapsulation process [34]. The process commenced by blending 200 mL of pure water, a minuscule quantity of ammonia (0.1 mL), and 5.5 g of Tween 80, which were constantly mixed for roughly 15 min. Next, the pH level was gauged and regulated to 9.0, and subsequently, 1-butanol was added, and its mixture was again stirred for an extra 5 min [35]. The solution was then transferred to a reactor enclosed by aluminum foil, and 15 mL of SF was blended in and mixed at 320 rpm and 27 °C for one hour. Afterward, 2 mL of TEVS was added and stirred under the same conditions for 20 h. The solution was further cleared of nanoparticles through

dialysis using a dialysis membrane, with the duration depending on the concentration of the photosensitizer [34].

SiNPs enclosed six different concentrations of SF at diverse final concentrations as stated in [36], specifically 52.0, 26.0, 13.0, 6.5, 3.3, and 1.6  $\mu\text{M}$ . MCF-7 (HTB-22 from ATCC) procured from the minus 80 °C freezer were mixed with 6 mL of DMEM medium in a 15 mL plastic tube and later centrifuged at 2000 rpm for 15 min. The cells, now concentrated and cleaned, settled at the bottom of the centrifuge tube. The MCF-7 cell culture in DMEM medium was treated with 1% antibiotic (penicillin) and 10% fetal bovine serum for six hours under 37 °C in a 5% CO<sub>2</sub> environment. The culture was then left overnight to allow cell growth. They were then washed three times with PBS and incubated with 5 mL of fresh DMEM medium containing SF-encapsulated SiNPs in all concentrations [35]. All the samples were exposed to the light source (intensity  $\sim 110 \text{ mW/cm}^2$  red laser, with a 40 cm distance between the sample and the laser source) for 60 min. The medium was removed, and the cells were rinsed twice with PBS solution. Fresh DMEM medium (3 mL) was added, and the cells were incubated overnight. The cytotoxicity and optimal concentration of SF-SiNPs were assessed via the MTT cell counting method; then, the previous protocol was repeated three times [36].

Silica nanoparticles were studied using Transmission Electron Microscopy (TEM) and a Malvern Nano-ZS90 particle size analyzer to perform morphological examinations. Progressive hydrodynamic size recordings were accomplished for SF-SiNPs over 0, 2, 4, and 6 days. Cell count calculations were executed with the use of an inverted light microscope and hemocytometers. The cells were suspended in 4 mL of fresh medium, and a blend of 10  $\mu\text{L}$  of cells and 10  $\mu\text{L}$  of trypan blue was incubated for 15 min. Then, 8  $\mu\text{L}$  of the combination was positioned onto the hemocytometer through a micropipette and covered with a coverslip. The hemocytometer was attached to the stage of the light microscope, and cell counting was performed on four squares, each containing 16 small squares. The bright cells counted were averaged, then multiplied by 104/4 to compute the cell count per ml of the suspension sample. Based on the total cell count, including both living and dead cells, cell viability was assessed. Two samples of cells were evaluated to gauge the cell viability. The first sample was untreated cells without exposure to any photosensitizer or light source and was used to determine the total number of untreated cells.

After undergoing PDT, the ratio of living cells in the second sample was calculated as a percentage compared to the untreated sample to determine cell viability [35]. The cytotoxicity of MCF-7 cells with encapsulated SF-SiNPs was assessed by comparing the number of untreated control cells to those treated with SF-SiNPs and incubated for 7 h without exposure to light in a controlled environment. The IC<sub>50</sub> was subsequently determined to measure the half-maximal inhibitory concentration.

The dead cell percentage was measured by performing MTT analysis on cells treated with SF-SiNPs at different concentrations (52.0, 26.0, 13.0, 6.5, 3.3, and 1.6  $\mu\text{M}$ ). The optimal concentration was determined before subjecting it to varying exposure durations ranging between 0 to 90 min to ascertain the ideal duration. Similarly, naked SF was also tested for its efficacy over 60 min at the optimal concentration with varying exposure at (0, 15, 30, 45, 60, 75, and 90 min). The efficacy equation was used to compare the concentration and exposure time effectiveness of SF-SiNPs against naked SF [37]:

$$\text{CE} = [(C_{\text{encapsulated}} - C_{\text{naked}})/C_{\text{encapsulated}}] \times 100\% \quad (1)$$

where CE is the concentration efficacy,  $C_{\text{encapsulated}}$  is the concentration of encapsulated SF, and  $C_{\text{naked}}$  is the concentration of naked SF. Additionally, we used the same method to measure the exposure time efficacy.

### 3. Results and Discussion

#### 3.1. Characterization of the SF-SiNPs

Figure 1 presents the UV-vis spectrophotometer spectrum of naked SF, providing valuable insights into its optical properties. The spectrum clearly indicates that SF demon-

strated a maximum peak absorbance at 512 nm, signifying its strong absorption within the desired range for effective photodynamic therapy. For the subsequent experiment, a red laser radiation source with a power intensity of  $110 \text{ mW}/\text{cm}^2$  was utilized. The sample was positioned at a 40 cm from the radiation source, ensuring appropriate exposure conditions for the photodynamic therapy procedure. These parameters were carefully selected to optimize the therapeutic outcome of the experiment.

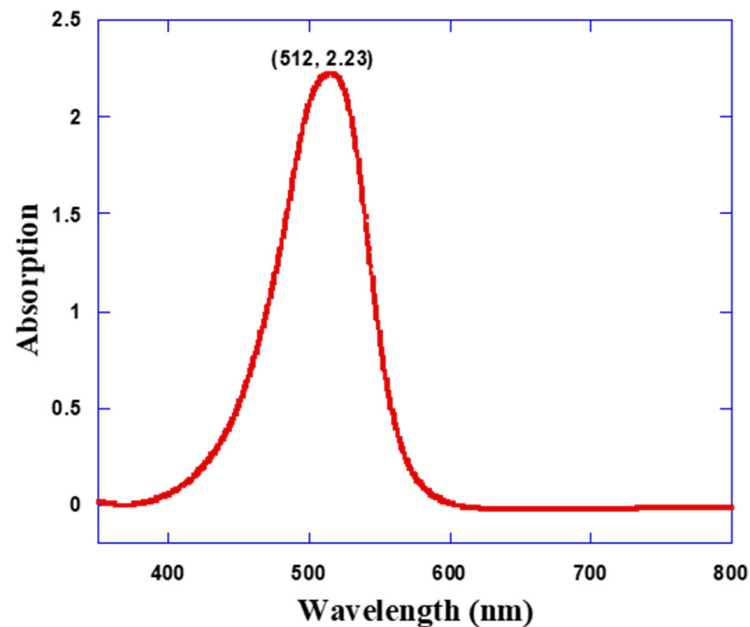


**Figure 1.** UV-vis Spectrophotometer Spectrum of free SF.

To validate the morphological characteristics and particle sizes of the SF-SiNPs, transmission electron microscopy (TEM), micrographs were employed and presented in Figure 2. The micrographs provided visual evidence of the well-dispersed spherical shape of the encapsulated SF within SiNPs. Through two-dimensional imaging analysis, the average diameter of the SF-SiNPs was determined to be approximately 30 nm. These observations confirm the successful encapsulation of SF within SiNPs and provide crucial information regarding the size and structure of the composite particles.

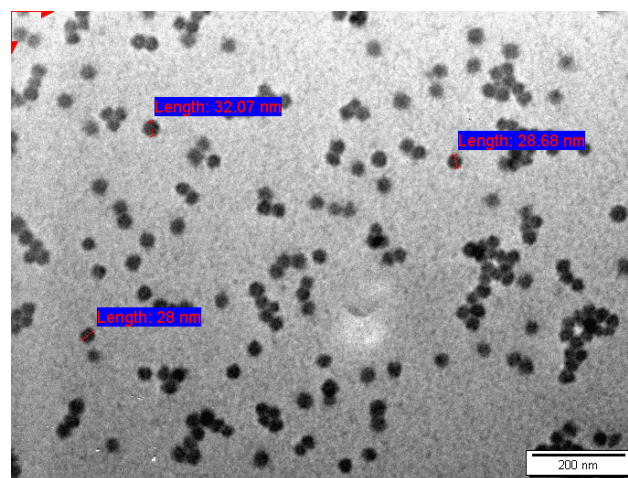


**Figure 2.** TEM visualization and analysis of SF encapsulated by SiNPs.

The stability of the SiNPs was carefully evaluated by measuring their hydrodynamic size using a zeta-sizer machine over six days after their synthesis. Figure 3 illustrates the

results, demonstrating that the average size of the SiNPs remained relatively constant at approximately 31 nm throughout the measurement period. Notably, no precipitate was observed, and the suspended solution exhibited no significant alteration in size. These findings indicate that the SF-SiNPs exhibited remarkable stability over the course of the treatment duration [38,39]. The observed stability of the SiNPs is crucial for their effective utilization as carriers for SF in photodynamic therapy applications. When the encapsulated PS was purified using a dialysis membrane for several days, the exchanged water was found to be pure, indicating that free safranin was not present. This finding demonstrates the effective encapsulation of safranin within the silica nanoparticles and its stability post-purification. Hence, it can be concluded that all safranin within the PS was successfully encapsulated and maintained in a stable state.

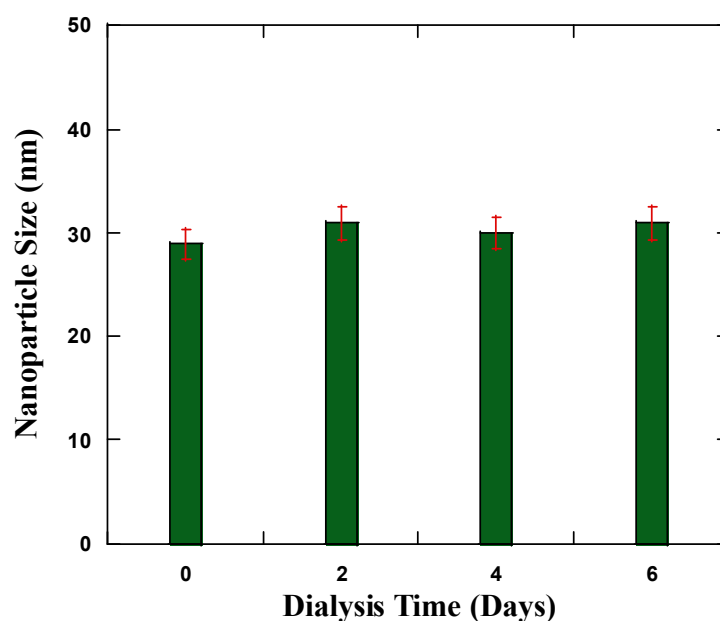


**Figure 3.** Particle size analysis of the SiNPs several times during the first 6 days.

### 3.2. Cytotoxicity of Naked and Encapsulated SF on MCF-7 Cells

To assess the effects of photodynamic therapy *in vitro*, the cytotoxic effects of SF needed to be evaluated on MCF-7 cells. Figure 4a illustrates the cytotoxicity of pure SiNPs, indicating that there was no significant toxic effect observed after 24 h of incubation. The evaluation involved incubating the cells with various concentrations of naked and encapsulated SF. The cytotoxicity was demonstrated in Figure 4 through five different concentrations (52.0, 26.0, 13.0, 6.5, 3.3, and 1.6  $\mu\text{M}$ ) of both SF formulations. It was observed that  $\text{IC}_{50}$  values for both formulations were lower than 13  $\mu\text{M}$ , indicating their potential to induce cytotoxicity in MCF-7 cells. These results endorse the promise of both formulations as photodynamic therapy candidates for treating breast cancer.

Encapsulated SF was observed to have increased cytotoxicity compared to naked SF, which can be attributed to the presence of silica nanoparticles on its outer surface. It is imperative to consider the physicochemical properties of SiNPs and the type of cell being targeted when evaluating their cytotoxicity [40]. The presence of certain chemicals on the outer surface of SiNPs may also contribute to their cytotoxic effects such as 1-butanol and Tween 80. Figure 4b illustrates that encapsulated and naked SF can be effectively used to achieve desired cytotoxic effects at concentrations below 13 mM.

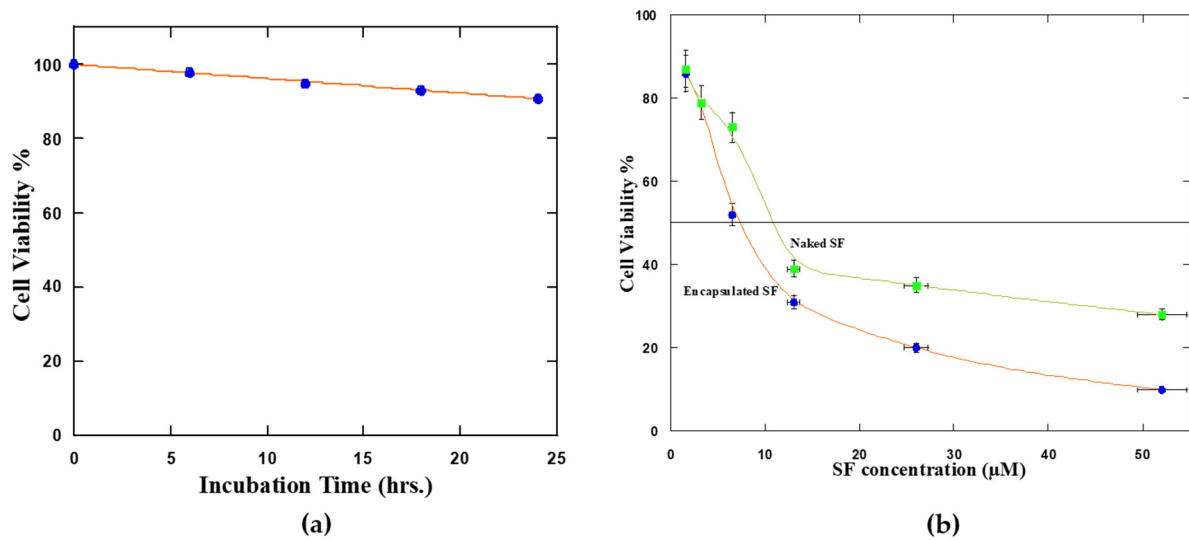


**Figure 4.** (a) Cytotoxicity measurements of pure SiNPs on MCF-7 for 24 h incubation. (b) Cytotoxicity of naked (green color) and encapsulated SF (red color) on MCF-7 cells at different concentrations.

3.3. The Optimal Concentration of Encapsulated and Naked SF

The SF-SiNPs were tested on MCF-7 cells at varying concentrations (52.0, 26.0, 13.0, 6.5, 3.3, and 1.6 µM) using a hemocytometer to determine the number of dead cells. The results in Figure 5 show the percentage of cell death for both naked and encapsulated SF under different light exposure conditions. Samples that were exposed to light underwent continuous irradiation for an hour.

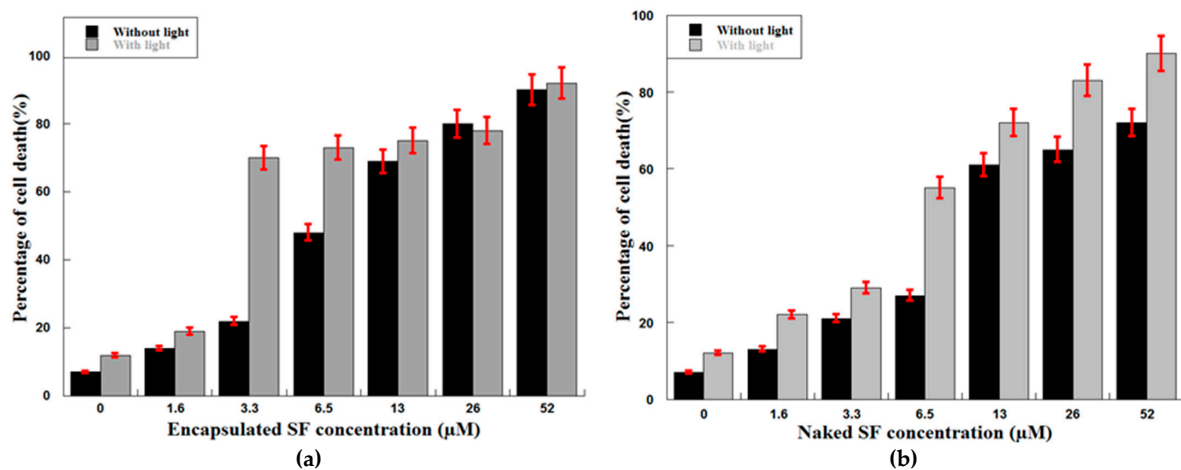


**Figure 5.** Comparison of cell death percentage with and without irradiation for (a) encapsulated SF and (b) naked SF.

Figure 5a reveals that when SF-SiNPs were introduced to MCF-7 cells without light at concentrations of 52.0, 26.0, and 13.0 M, over 50% cytotoxicity was observed. However, when the same SF-SiNPs were exposed to light at concentrations of 52.0, 26.0, 13.0, 6.5, and 3.3 M, more than half of the cells were eliminated. The efficacy of SF-SiNPs at 3.3 M was demonstrated in Figure 6 by examining the difference in dead cell percentage under light and dark conditions. Under dark conditions, naked SF showed a cytotoxic level of over 50% at 52.0, 26.0, and 13.0 m. However, naked SF killed over 50% of cells at 52.0, 26.0, 13.0, and 6.5 M concentrations, as shown in Figure 5b. The dead cell percentage ratio when comparing light irradiation to dark conditions provided evidence that the ideal concentration for the naked SF, yielding the maximum ratio, was 6.5 µM, as depicted in Figure 6. The results suggest that the concentration of encapsulated SF required to achieve

a similar level of cell destruction in MCF-7 cells is roughly half that of naked SF. As a result, the concentration efficacy was calculated to be 50% using the efficacy equation.

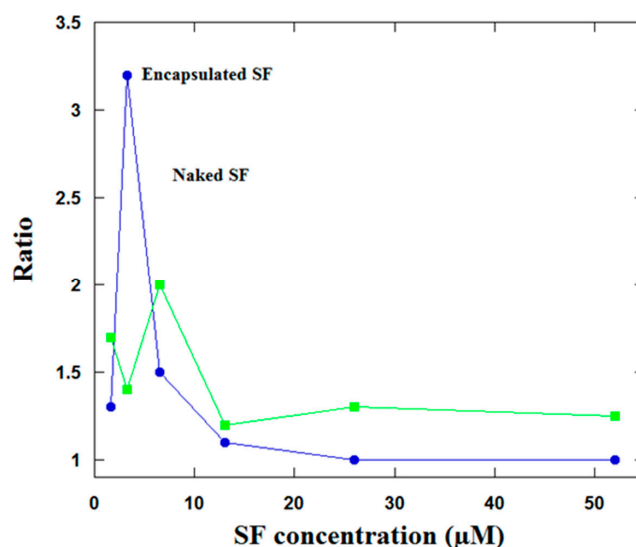


**Figure 6.** The ratio of percentage cell death under light irradiation to that without light irradiation for encapsulated (blue color) and naked SF (green color).

Nevertheless, the cell death percentage rose as the concentration of encapsulated and naked SF increased during light exposure due to the production of singlet oxygen or ROS resulting from SF's exposure to light [35]. Furthermore, the cytotoxicity generated in the absence of light was elevated as the concentration of SF increased.

#### 3.4. The Optimal Exposure Time for Encapsulated and Naked SF

The previous section concluded the ideal concentrations necessary to evaluate the time-dependent repercussions of treatment on both encapsulated and naked SF. MCF-7 cells underwent treatment with 3.3 µM and 6.5 µM of encapsulated and naked SF, respectively. Encapsulated SF underwent exposure to light for varying time spans (0, 15, 30, 45, 60, 75, and 90 min), as apparent in Figure 7a. Figure 7c revealed nearly 28 min as the optimal duration required to eliminate 50% of the MCF-7 cells employing encapsulated SF, whereas the same durations showed that 50% of the cells were destroyed post-50 min with naked SF (Figure 7c). As such, encapsulated SF was more effective at destroying the target cells than naked SF, requiring less exposure time. Therefore, the exposure time efficacy was calculated to be 78% using the efficacy equation.

Figure 8 displays microscope images of MCF-7 cells subjected to photodynamic therapy using naked and encapsulated SF at various exposure times. The images highlight the contrasting efficacy of the two types of SF.

The photodynamic effect required a lower concentration of encapsulated SF to achieve the same level of toxicity compared to naked SF as a treatment for MCF-7 cells. However, the photodynamic effect by naked SF necessitated more irradiation time to destroy half of the target cells at the optimal SF concentration than the encapsulated SF. The use of light irradiation resulted in effective damage to cancer cells, which was attributed to the ability of encapsulated SF molecules to absorb more light and generate singlet oxygen in ROS [41]. This was due to the clustering of SF molecules in SiNPs through encapsulation, in contrast to naked SF, which was dispersed in the solution and had weaker interactions with light, leading to less effective damage [33,41].

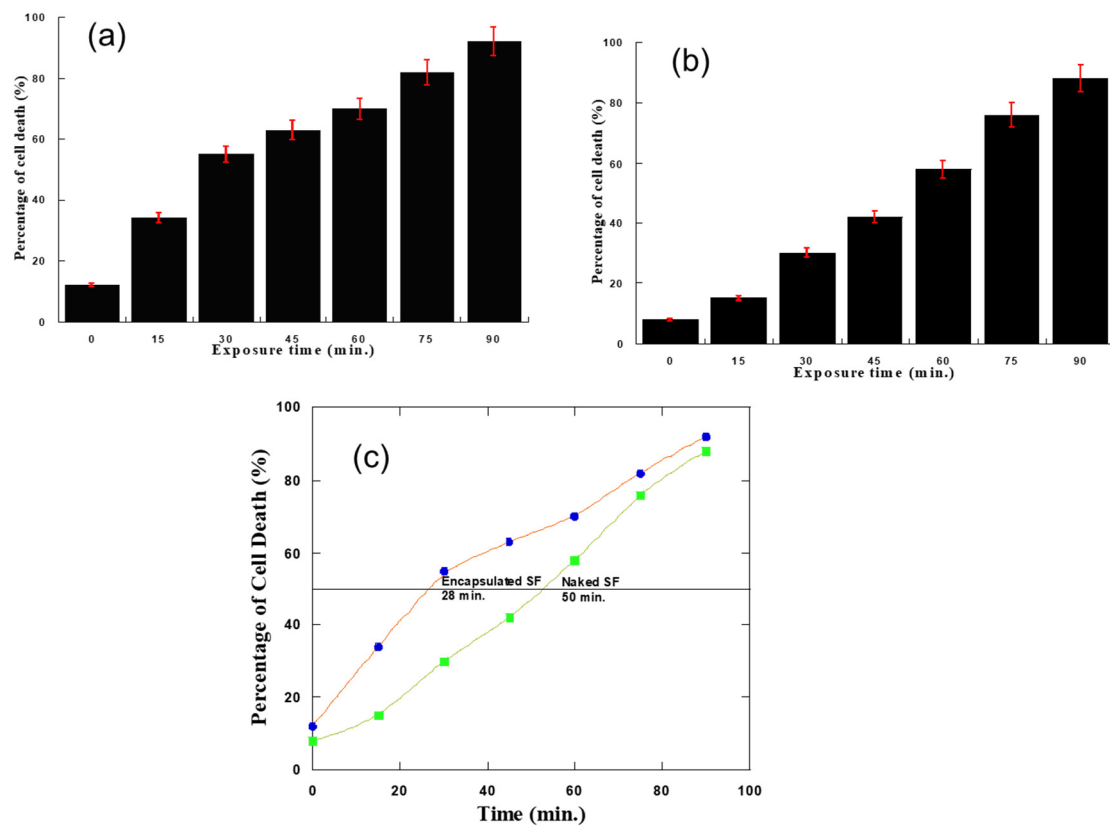


Figure 7. The time dependence of the treatment by using the optimal concentration for (a) encapsulated SF (red color) and (b) naked SF (green color). (c) The optimum exposure time for the treatment.

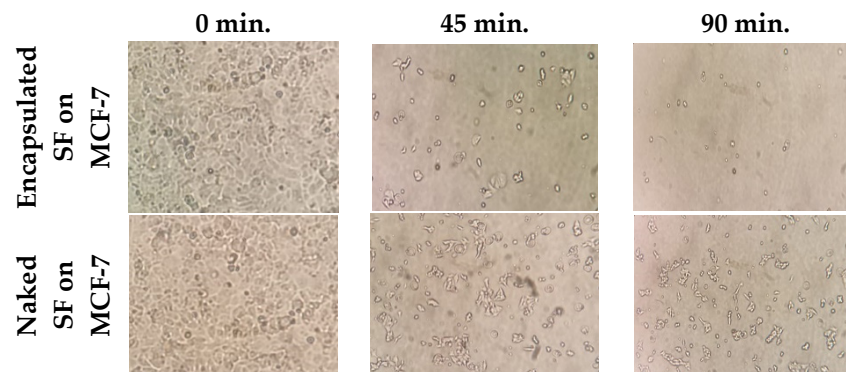


Figure 8. Microscope images of MCF-7 during treatment using encapsulated and naked SF for different exposure times.

#### 4. Conclusions

In conclusion, the study reveals that encapsulation of SiNPs improves SF therapeutic efficacy in MCF-7 photodynamic therapy. This result shows that the use of SiNPs can be a promising approach to the treatment of breast cancer. Furthermore, it is suggested that the combination of SiNPs and SF can be a more effective and safe choice for cancer photodynamic therapy. As a result of enhanced light accessibility, encapsulated SF produces higher ROS levels and displays enhanced PDT efficacy compared to naked SF. Moreover, encapsulated SF exhibits an optimal treatment concentration of 3.3  $\mu\text{M}$ , reducing exposure time to only 28 min compared to 50 min for naked SF. The results of this study demonstrate the potential of encapsulated SF as a treatment for cancer that is more targeted and efficient. Furthermore, the study provides valuable insights into the promising use of nanotechnology to improve the effectiveness of photosensitizing agents. As a result, cancer treatments are

enhanced with fewer side effects. The findings of this study have significant implications for how cancer treatments are designed and administered. This research could lead to better and more targeted treatments for cancer that are more effective and less damaging to the body. This opens up new avenues for nanotechnology-driven approaches to cancer treatment that have the potential to be more effective.

**Author Contributions:** Funding acquisition, K.A. and M.-A.H.A.-A.; Investigation, K.A., M.-A.H.A.-A., G.N.M. and T.A.; Supervision, K.A. and M.-A.H.A.-A.; Project administration, K.A. and M.-A.H.A.-A.; Writing—review & editing, K.A., M.-A.H.A.-A., G.N.M., T.A., S.H.Z., M.H.A.M. and O.A.N.; Writing—original draft, G.N.M. and T.A.; Methodology, G.N.M., K.A. and T.A.; Formal analysis, G.N.M., O.A.N., T.A., S.H.Z. and M.M.M.; Conceptualization, G.N.M., K.A. and T.A.; Data curation, G.N.M.; Visualization, G.N.M., O.A.N. and T.A.; Validation, K.A., M.-A.H.A.-A., G.N.M., T.A., S.H.Z., M.H.A.M., M.M.M. and O.A.N. All authors have read and agreed to the published version of the manuscript.

**Funding:** The authors would like to thank the Deanship of Research at Jordan University of Science and Technology for supporting and funding this research project (Grant # 20220582).

**Data Availability Statement:** Data available on request.

**Conflicts of Interest:** The authors declare no conflict of interest.

## References

- Schuitmaker, J.J.; Baas, P.; van Leengoed, H.L.; van der Meulen, F.W.; Star, W.M.; van Zandwijk, N. Photodynamic therapy: A promising new modality for the treatment of cancer. *J. Photochem. Photobiol. B Biol.* **1996**, *34*, 3–12. [[CrossRef](#)] [[PubMed](#)]
- Zhao, X.; Liu, J.; Fan, J.; Chao, H.; Peng, X. Recent progress in photosensitizers for overcoming the challenges of photodynamic therapy: From molecular design to application. *Chem. Soc. Rev.* **2021**, *50*, 4185–4219. [[CrossRef](#)] [[PubMed](#)]
- Al Akhras, M.A.H.; Aljarrah, K.; Makhadmeh, G.N.; Shorman, A. Introducing the Effect of Chinese Chlorella as a Photosensitizing Drug at Different Temperatures. *J. Mol. Pharm. Org. Process. Res.* **2013**, *1*, e109. [[CrossRef](#)]
- Ji, C.; Li, H.; Zhang, L.; Wang, P.; Lv, Y.; Sun, Z.; Tan, J.; Yuan, Q.; Tan, W. Ferrocene-Containing Nucleic Acid-Based Energy-Storage Nanoagent for Continuously Photo-Induced Oxidative Stress Amplification. *Angew. Chem. Int. Ed.* **2022**, *61*, e202200237. [[CrossRef](#)] [[PubMed](#)]
- Tang, W.; Xu, H.; Park, E.J.; Philbert, M.A.; Kopelman, R. Encapsulation of methylene blue in polyacrylamide nanoparticle platforms protects its photodynamic effectiveness. *Biochem. Biophys. Res. Commun.* **2008**, *369*, 579–583. [[CrossRef](#)]
- Wilczewska, A.Z.; Niemirowicz, K.; Markiewicz, K.H.; Car, H. Nanoparticles as drug delivery systems. *Pharmacol. Rep.* **2012**, *64*, 1020–1037. [[CrossRef](#)]
- Abuelsamen, A.; Mahmud, S.; Kaus, N.H.M.; Farhat, O.F.; Mohammad, S.M.; Al-Suede, F.S.R.; Majid, A.M.S.A. Novel Pluronic F-127-coated ZnO nanoparticles: Synthesis, characterization, and their in-vitro cytotoxicity evaluation. *Polym. Adv. Technol.* **2021**, *32*, 2541–2551. [[CrossRef](#)]
- Xiong, R.; Hua, D.; Van Hoeck, J.; Berdecka, D.; Léger, L.; De Munter, S.; Fraire, J.C.; Raes, L.; Harizaj, A.; Sauvage, F.; et al. Photothermal nanofibres enable safe engineering of therapeutic cells. *Nat. Nanotechnol.* **2021**, *16*, 1281–1291. [[CrossRef](#)]
- Bharali, D.J.; Klejbor, I.; Stachowiak, E.K.; Dutta, P.; Roy, I.; Kaur, N.; Bergey, E.J.; Prasad, P.N.; Stachowiak, M.K. Organically modified silica nanoparticles: A nonviral vector for in vivo gene delivery and expression in the brain. *Proc. Natl. Acad. Sci. USA* **2005**, *102*, 11539–11544. [[CrossRef](#)]
- Xiong, R.; Xu, R.X.; Huang, C.; De Smedt, S.; Braeckmans, K. Stimuli-responsive nanobubbles for biomedical applications. *Chem. Soc. Rev.* **2021**, *50*, 5746–5776. [[CrossRef](#)]
- Kneuer, C.; Sameti, M.; Haltner, E.G.; Schiestel, T.; Schirra, H.; Schmidt, H.; Lehr, C.-M. Silica nanoparticles modified with aminosilanes as carriers for plasmid DNA. *Int. J. Pharm.* **2000**, *196*, 257–261. [[CrossRef](#)] [[PubMed](#)]
- Santra, S.; Yang, H.; Dutta, D.; Stanley, J.T.; Holloway, P.H.; Tan, W.; Moudgil, B.M.; Mericle, R.A. TAT conjugated, FITC doped silica nanoparticles for bioimaging applications. *Chem. Commun.* **2004**, 2810–2811. [[CrossRef](#)] [[PubMed](#)]
- Ma, Q.; Sun, X.; Wang, W.; Yang, D.; Yang, C.; Shen, Q.; Shao, J. Diketopyrrolopyrrole-derived organic small molecular dyes for tumor phototheranostics. *Chin. Chem. Lett.* **2021**, *33*, 1681–1692. [[CrossRef](#)]
- Alzoubi, F.; Abu Noqta, O.; AlZoubi, T.; AlJabaly, H.; Alkhateeb, H.; Alqadi, M.; Makhadmeh, G. Exploring the impact of pH on the properties of citric acid-coated iron oxide nanoparticles as high-performance T2 contrast agent for MRI applications. *Results Eng.* **2023**, *18*, 101206. [[CrossRef](#)]
- Rad, A.T.; Chen, C.-W.; Aresh, W.; Xia, Y.; Lai, P.-S.; Nieh, M.-P. Combinational Effects of Active Targeting, Shape, and Enhanced Permeability and Retention for Cancer Theranostic Nanocarriers. *ACS Appl. Mater. Interfaces* **2019**, *11*, 10505–10519. [[CrossRef](#)]
- Iturrioz-Rodríguez, N.; Correa-Duarte, M.A.; Fanarraga, M.L. Controlled drug delivery systems for cancer based on mesoporous silica nanoparticles. *Int. J. Nanomed.* **2019**, *14*, 3389–3401. [[CrossRef](#)]
- Abd-El-Aziz, H.S.; Habit, A.T. The Toxicity Effect of Certain Photosensitizing Compounds on Some Biological Aspects of Field Strain of *Agrotis ipsilon* (Hufnagel) Larvae. *Egypt. Acad. J. Biol. Sci. F Toxicol. Pest Control* **2021**, *13*, 195–208. [[CrossRef](#)]

18. Saha, I.; Kumar, G.S. Spectroscopic Characterization of the Interaction of Phenosafranin and Safranin O with Double Stranded, Heat Denatured and Single Stranded Calf Thymus DNA. *J. Fluoresc.* **2010**, *21*, 247–255. [[CrossRef](#)]
19. Kenley, R.A.; Kirshen, N.A.; Mill, T. Photooxidation of Di-n-butyl Sulfide Using Sensitizers Immobilized in Polymer Films. *Macromolecules* **1980**, *13*, 808–815. [[CrossRef](#)]
20. Zweig, A.; Henderson, W.A., Jr. Singlet oxygen and polymer photooxidations. I. Sensitizers, quenchers, and reactants. *J. Polym. Sci. Polym. Chem. Ed.* **1975**, *13*, 717–736. [[CrossRef](#)]
21. Albiter, E.; Alfaro, S.; Valenzuela, M.A. Photosensitized Oxidation of 9,10-Dimethylanthracene on Dye-Doped Silica Composites. *Int. J. Photoenergy* **2012**, *2012*, 987606. [[CrossRef](#)]
22. Kaur, S.; Rani, S.; Mahajan, R.; Asif, M.; Gupta, V.K. Synthesis and adsorption properties of mesoporous material for the removal of dye safranin: Kinetics, equilibrium, and thermodynamics. *J. Ind. Eng. Chem.* **2014**, *22*, 19–27. [[CrossRef](#)]
23. Malekbala, M.R.; Hosseini, S.; Yazdi, S.K.; Soltani, S.M.; Malekbala, M.R. The study of the potential capability of sugar beet pulp on the removal efficiency of two cationic dyes. *Chem. Eng. Res. Des.* **2012**, *90*, 704–712. [[CrossRef](#)]
24. Shariati, S.; Faraji, M.; Yamini, Y.; Rajabi, A.A. Fe<sub>3</sub>O<sub>4</sub> magnetic nanoparticles modified with sodium dodecyl sulfate for removal of safranin O dye from aqueous solutions. *Desalination* **2011**, *270*, 160–165. [[CrossRef](#)]
25. Beech, S.J.; Noimark, S.; Page, K.; Noor, N.; Allan, E.; Parkin, I.P. Incorporation of crystal violet, methylene blue and safranin O into a copolymer emulsion; the development of a novel antimicrobial paint. *RSC Adv.* **2015**, *5*, 26364–26375. [[CrossRef](#)]
26. Jankowski, A.; Jankowski, S.; Mirończyk, A.; Niedbach, J. The action of photosensitizers and serum in a bactericidal process. II. The effects of dyes: Hypericin, eosin Y and safranin O. *Pol. J. Microbiol.* **2005**, *54*, 323–330.
27. Voos, A.C.; Kranz, S.; Tonndorf-Martini, S.; Voelpel, A.; Sigusch, H.; Staudte, H.; Albrecht, V.; Sigusch, B.W. Photodynamic antimicrobial effect of safranin O on an ex vivo periodontal biofilm. *Lasers Surg. Med.* **2014**, *46*, 235–243. [[CrossRef](#)] [[PubMed](#)]
28. Sasnauskienė, A.; Kadziauskas, J.; Vezelyte, N.; Jonusienė, V.; Kirveliėnė, V. Apoptosis, autophagy and cell cycle arrest following photodamage to mitochondrial interior. *Apoptosis* **2009**, *14*, 276–286. [[CrossRef](#)]
29. Mekki, A.I.; Eleraky, N.E.; Soliman, G.M.; Elnaggar, M.G.; Elnaggar, M.G. Combinatorial Therapy of Letrozole- and Quercetin-Loaded Spanlastics for Enhanced Cytotoxicity against MCF-7 Breast Cancer Cells. *Pharmaceutics* **2022**, *14*, 1727. [[CrossRef](#)]
30. Bielack, S.S.; Kempf-Bielack, B.; Dellling, G.; Exner, G.U.; Flege, S.; Helmke, K.; Kotz, R.; Salzer-Kuntschik, M.; Werner, M.; Winkelmann, W.; et al. Prognostic Factors in High-Grade Osteosarcoma of the Extremities or Trunk: An Analysis of 1,702 Patients Treated on Neoadjuvant Cooperative Osteosarcoma Study Group Protocols. *J. Clin. Oncol.* **2002**, *20*, 776–790. [[CrossRef](#)]
31. Whelan, J.S.; Jinks, R.C.; McTiernan, A.; Sydes, M.R.; Hook, J.M.; Trani, L.; Uscinska, B.; Bramwell, V.; Lewis, I.J.; Nooij, M.A.; et al. Survival from high-grade localised extremity osteosarcoma: Combined results and prognostic factors from three European Osteosarcoma Intergroup randomised controlled trials. *Ann. Oncol.* **2012**, *23*, 1607–1616. [[CrossRef](#)]
32. Prathyusha, E.; Prabakaran, A.; Ahmed, H.; Dethle, M.R.; Agrawal, M.; Gangipangi, V.; Sudhagar, S.; Krishna, K.V.; Dubey, S.K.; Pemmaraju, D.B.; et al. Investigation of ROS generating capacity of curcumin-loaded liposomes and its in vitro cytotoxicity on MCF-7 cell lines using photodynamic therapy. *Photodiagn. Photodyn. Ther.* **2022**, *40*, 103091. [[CrossRef](#)] [[PubMed](#)]
33. Roy, I.; Ohulchanskyy, T.Y.; Pudavar, H.E.; Bergey, E.J.; Oseroff, A.R.; Morgan, J.; Dougherty, T.J.; Prasad, P.N. Ceramic-Based Nanoparticles Entrapping Water-Insoluble Photosensitizing Anticancer Drugs: A Novel Drug-Carrier System for Photodynamic Therapy. *J. Am. Chem. Soc.* **2003**, *125*, 7860–7865. [[CrossRef](#)] [[PubMed](#)]
34. Chatterjee, D.K.; Fong, L.S.; Zhang, Y. Nanoparticles in photodynamic therapy: An emerging paradigm. *Adv. Drug Deliv. Rev.* **2008**, *60*, 1627–1637. [[CrossRef](#)] [[PubMed](#)]
35. Makhadmeh, G.N.; Abuelsamen, A.; Al-Akhras, M.-A.H.; Aziz, A.A. Silica Nanoparticles Encapsulated Cichorium Puntillatum as a Promising Photosensitizer for Osteosarcoma Photodynamic Therapy: In-vitro study. *Photodiagn. Photodyn. Ther.* **2022**, *38*, 102801. [[CrossRef](#)]
36. Makhadmeh, G.N.; Aziz, A.A.; Razak, K.A.; Abu Noqta, O. Encapsulation efficacy of natural and synthetic photosensitizers by silica nanoparticles for photodynamic applications. *IET Nanobiotechnol.* **2015**, *9*, 381–385. [[CrossRef](#)]
37. Erickson, A.J.; Weiss, P.T.; Gulliver, J.S. *Stormwater Treatment: Assessment and Maintenance*; St. Anthony Falls Laboratory: Minneapolis, MN, USA, 2010.
38. Aditya, A.; Chattopadhyay, S.; Jha, D.; Gautam, H.K.; Maiti, S.; Ganguli, M. Zinc Oxide Nanoparticles Dispersed in Ionic Liquids Show High Antimicrobial Efficacy to Skin-Specific Bacteria. *ACS Appl. Mater. Interfaces* **2018**, *10*, 15401–15411. [[CrossRef](#)]
39. Chen, L.; Liu, J.; Zhang, Y.; Zhang, G.; Kang, Y.; Chen, A.; Feng, X.; Shao, L. The toxicity of silica nanoparticles to the immune system. *Nanomedicine* **2018**, *13*, 1939–1962. [[CrossRef](#)]
40. Al Jarrah, K.; Al-Akhras, M.-A.H.; Makhadmeh, G.N.; AlZoubi, T.; Abuelsamen, A.; Zyoud, S.H.; Mhareb, M.A.; Aziz, A.A.; Abu Noqta, O. A Novel Approach for Enhanced Osteosarcoma Photodynamic Therapy Using Encapsulated Methylene Blue in Silica Nanoparticles. *J. Compos. Sci.* **2023**, *7*, 137. [[CrossRef](#)]
41. Makhadmeh, G.N.; Abdul Aziz, A. Photodynamic application of protoporphyrin IX as a photosensitizer encapsulated by silica nanoparticles. *Artif. Cells Nanomed. Biotechnol.* **2018**, *46*, S1043–S1046. [[CrossRef](#)]

**Disclaimer/Publisher’s Note:** The statements, opinions and data contained in all publications are solely those of the individual author(s) and contributor(s) and not of MDPI and/or the editor(s). MDPI and/or the editor(s) disclaim responsibility for any injury to people or property resulting from any ideas, methods, instructions or products referred to in the content.